Wave propagation (MCSE)

Centrale Méditerranée

Homework 3

Presented by: SHARON DANIELA CASTRO BLANCO

Computed functions and plotting analysis in Matlab .

2. Collins formula.

(d) Numerical computation using the 2D FFT.

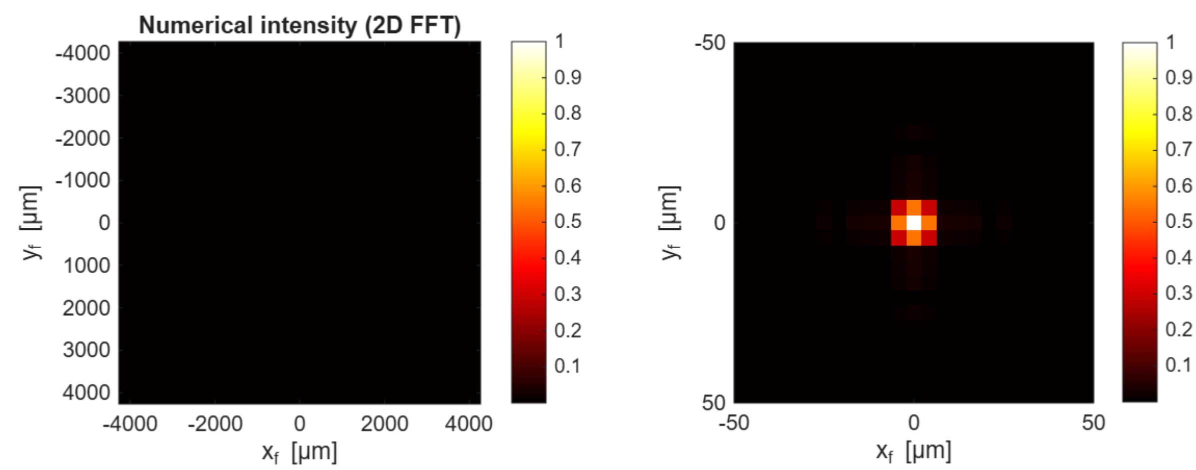

Figure 1. 2D FFT.
Source. Matlab

See code of the plot in: hmw2d.m

As we developed considering, we conclude that:

The analytical and numerical results are in very good agreement. Both methods show that a **2F optical system** performs a **2D Fourier Transform** of the aperture function.
For a square aperture of 5 mm side, illuminated by a wavelength of 500 nm and focused by a 100 mm focal length lens:

- The **resulting intensity pattern** in the focal plane exhibits the expected **2D sinc² distribution**.
- The **central lobe** extends approximately **±10 µm** from the origin (total width ≈ 20 µm).
- The **FFT-based numerical computation** accurately reproduces the theoretical Fraunhofer diffraction pattern when proper sampling and scaling are applied.
- The central maximum is confined within approximately ±10 µm from the optical axis, in agreement with the analytical prediction $x_0 = \lambda f / a = 10\mu m$. When the entire ±4 mm range is displayed, the pattern appears dark because the diffracted energy is highly concentrated near the center.
- Zooming into the ±50 µm region reveals the expected 2D sinc² diffraction pattern and confirms that the 2F optical system performs a Fourier transform of the aperture field.

In summary, the simulation validates that the 2F optical setup acts as a Fourier transformer, and the 2D FFT is an efficient numerical tool to compute and visualize the resulting optical field.

3.

(a)

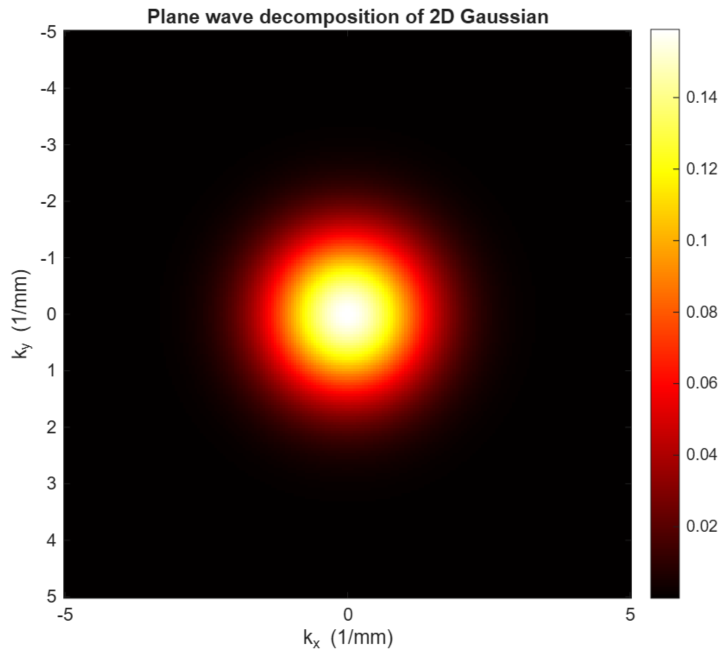

Figure 2. Plane wave of Gaussian TF.
Source. Matlab

See code of the plot in: hmw3a.m

The plane-wave decomposition (Fourier transform) of a Gaussian apodized mask is itself a Gaussian in k-space. With the forward transform convention used in class.

This result shows the well-known self-similarity of Gaussians under the Fourier transform: a narrow Gaussian in real space produces a broad Gaussian in k-space and vice versa. The analytical expression above is useful for propagation (multiply by the propagator $e^{ik_z(z_1-z_0)}$and inverse transform) and for quick estimates of beam angular or spatial-frequency content.

(b)

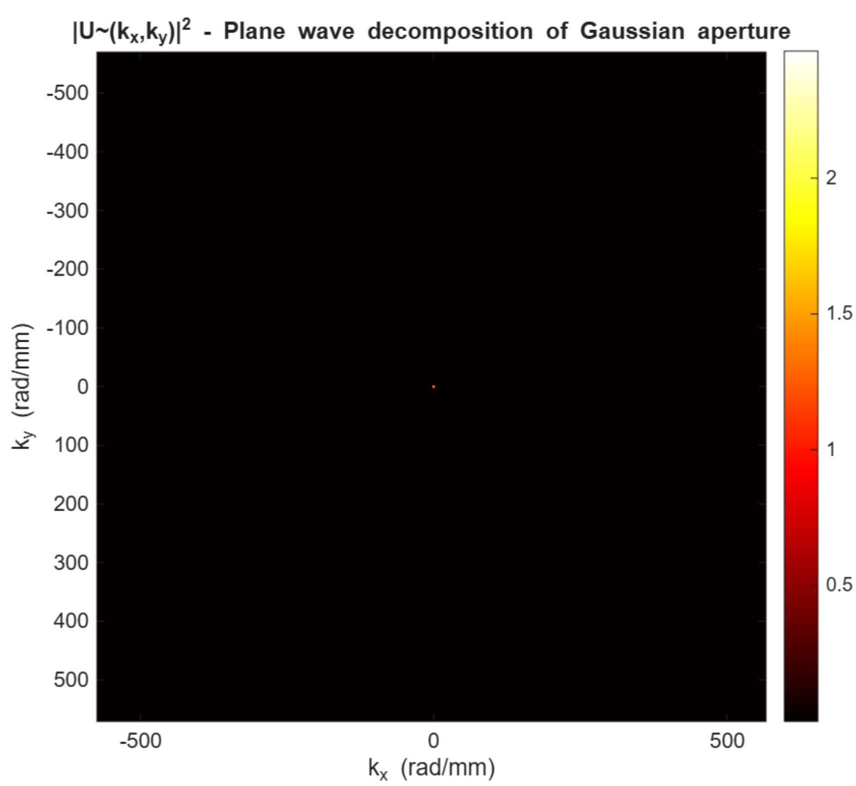

Figure 3. 2D FFT Gaussian Plane wave decomposition
Source. Matlab

See code of the plot in: hmw3b.m

The numerical 2D FFT of the Gaussian aperture with $\sigma = 0.5$ mm successfully computes the plane wave decomposition of the field. The resulting $|\tilde{U}(k_x, k_y)|^2$shows a Gaussian distribution in k-space, centered at $k_x = k_y = 0$, confirming that most of the field energy is carried by low spatial frequencies (near-normal plane waves). The width of the Gaussian in k-space is inversely proportional to the aperture size: smaller apertures lead to broader distributions of plane waves, while larger apertures concentrate energy near the center.

This numerical approach effectively demonstrates how the Fourier transform maps spatial structures into their plane wave components, providing a foundation for simulating field propagation using the plane wave method.

(c)

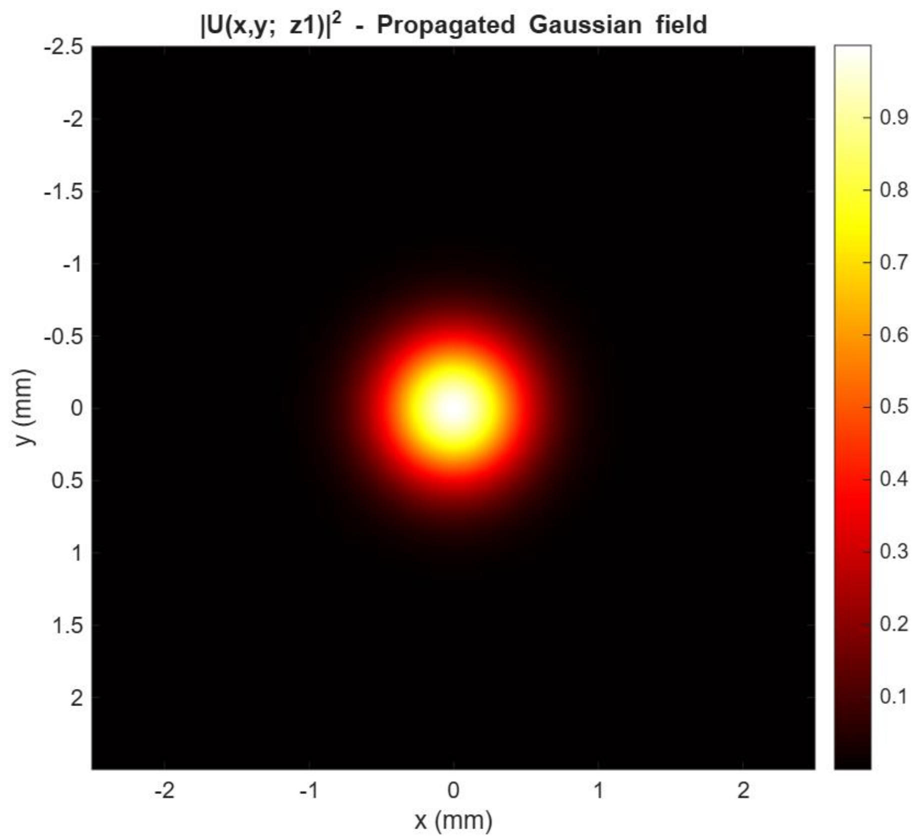

Figure 4. Graph of the Gaussian aperture (plane wave decomposition).
Source. Matlab

See code of the plot in: hmw3c.m

The numerical propagation of the Gaussian aperture over $z_1 - z_0 = 10$ mm using the plane wave decomposition shows that the field spreads slightly while maintaining its Gaussian shape. The intensity $|\ U(x, y; z_1)\ |^2$remains centered, but the beam width increases due to diffraction, illustrating the natural divergence of a Gaussian beam. This result confirms that the plane wave decomposition method accurately models free-space propagation: each plane wave accumulates a phase $e^{ik_z dz}$, and their coherent summation reproduces the expected diffraction-induced broadening in real space.

(d)

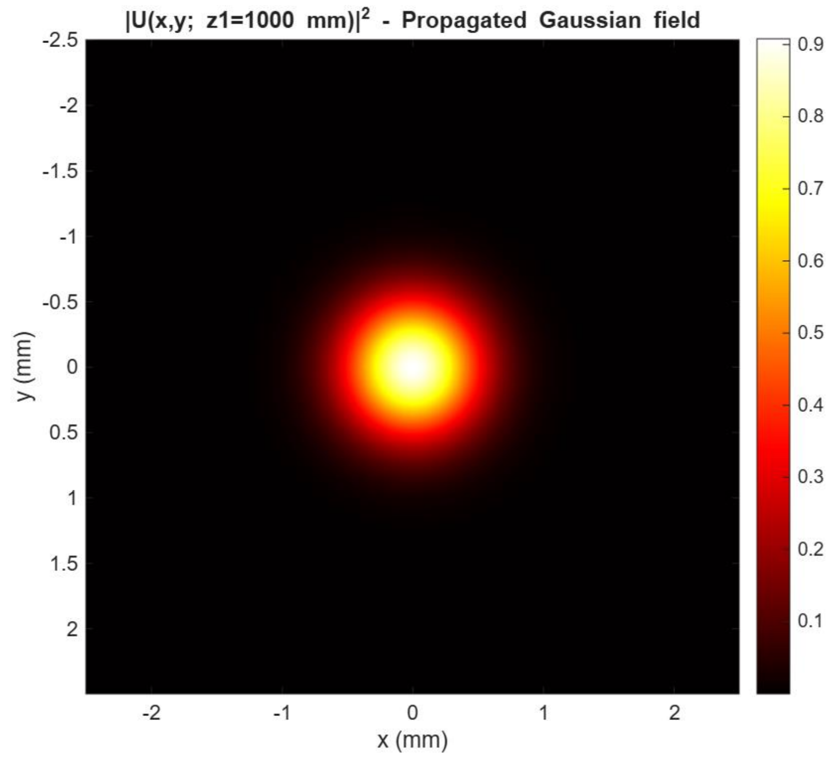

Figure 5. Graph of Gaussian Field propagated.
Source. Matlab

See code of the plot in: hmw3d.m

When the Gaussian field is propagated over a long distance of $z_1 - z_0 = 1000$ mm, the diffraction effect becomes much more pronounced. The intensity profile $|\, U(x, y; z_1) \,|^2$shows a significant increase in beam width and a corresponding decrease in peak intensity at the center. This demonstrates the divergent nature of Gaussian beams over long distances, as higher spatial frequencies in the plane wave decomposition spread more in space. The field maintains an approximately Gaussian shape, but it is much broader compared to short-distance propagation, illustrating the cumulative effect of free-space diffraction.

In other terms, numerically propagated Gaussian field ($\sigma = 0.5$ mm) over $z_1 - z_0 = 1000$ mm. The intensity $|\, U(x, y) \,|^2$ shows significant diffraction-induced broadening, with reduced peak intensity and an approximately Gaussian profile.

4.

(a)

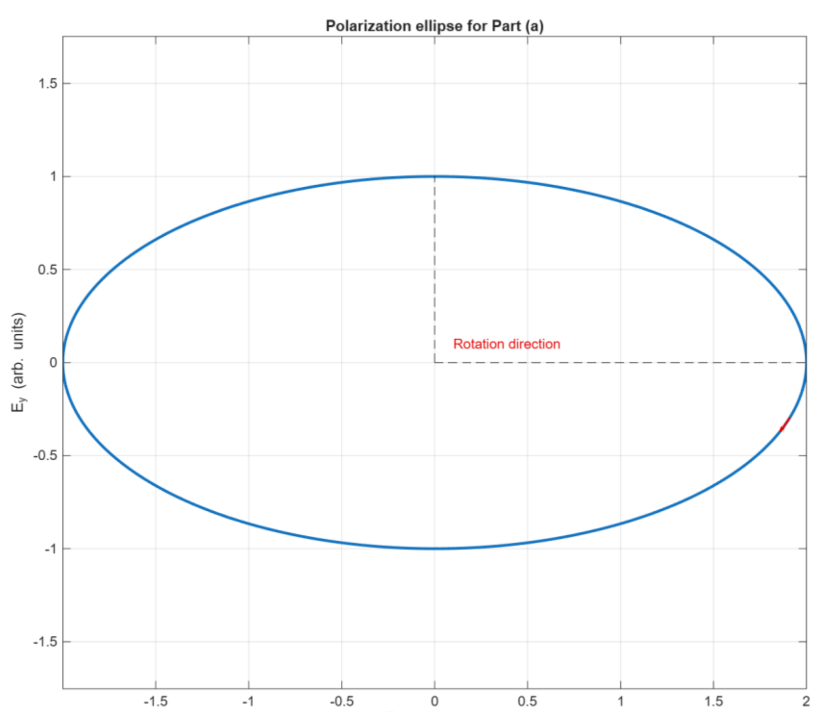

Figure 6. Graph of Jones vectors that describe three different elliptical polarizations.
Source. Matlab

See code of the plot in: hmw4a.m

In fact, the first vector (J_1 = [2; i]) corresponds to a left-handed (counterclockwise) ellipse, where the y-component lags the x-component by +90°. The second vector (J_2 = [2; -i]) represents a right-handed (clockwise) ellipse, with a -90° phase difference. The third vector (J_3 = (1/\sqrt{2})[2+i; -2+i]) produces an elliptically polarized wave tilted by 45° relative to the x-axis.

These Jones vectors describe how the amplitudes and relative phases of the electric field components determine the shape, orientation, and rotation direction of the polarization ellipse.

(b)

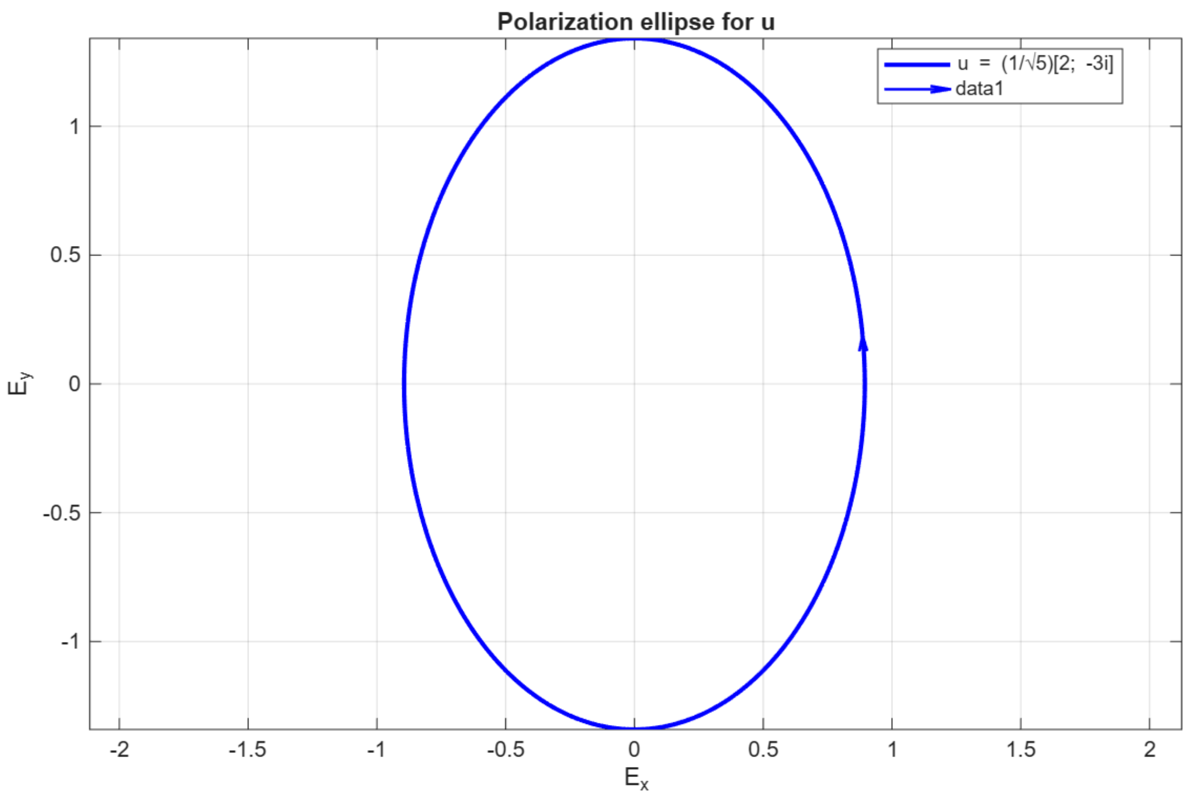

Figure 7. Graph of the orthogonal polarization state.
Source. Matlab

See code of the plot in: hmw4b.m

The orthogonal polarization state obtained from u $= \frac{1}{\sqrt{5}}(2, -3i)^T$ is v $= \frac{1}{\sqrt{5}}(-3i, 2)^T$. The plot of its polarization ellipse shows that this state has the same ellipse shape as the original polarization, but with its axes exchanged and the direction of rotation reversed. This reflects the definition of polarization orthogonality: the electric fields of the two states have zero inner product, meaning they share no common polarization component. Physically, an optical system aligned to transmit the first state will completely extinguish the orthogonal state. Thus, the plot confirms both the mathematical orthogonality and the geometric complementarity of the two polarization states.

The plot shows an ellipse elongated along the y-axis.

- The electric field vector rotates clockwise (right-handed), because the y-component lags the x-component by 90°.
- The semi-axes ratio $A_y/A_x = 3/2$ defines the ellipticity of the wave.

(c)

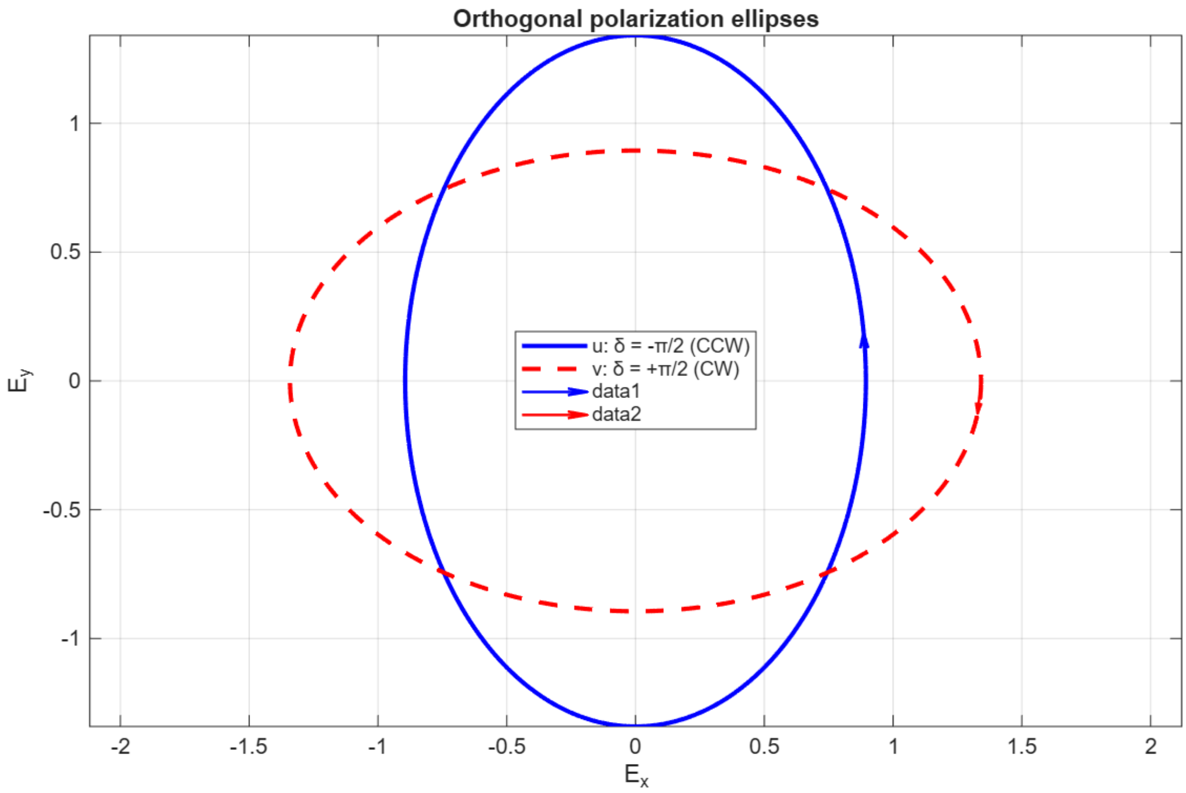

Figure 8. Graph of the orthogonal polarization state.
Source. Matlab

See code of the plot in: hmw4b.m

The plot of the orthogonal vector

$$v = \frac{1}{\sqrt{13}}\binom{-3i}{2}$$

displays another ellipse with the same shape but rotated in opposite direction.

- Here, the rotation is counterclockwise (left-handed) since the y-component leads the x-component by 90°.
- The two ellipses are orthogonal polarization states — identical geometry, opposite handedness.

This orthogonal state represents another elliptical polarization with the same shape but rotated 90° in phase space. Together, these two states form a pair of mutually orthogonal elliptical polarizations, completing a full polarization basis.